Showcasing research from Professor Arum Han's laboratory, Department of Electrical and Computer Engineering, Texas A&M University, USA.

Size-independent and automated single-colony-resolution microdroplet dispensing

This work introduces the first automated droplet dispensing platform capable of reliably achieving single-colony resolution under polydisperse conditions. By employing blank "spacer" droplets and a simple distance sensor, the system maintains separation between "hit" droplets during dispensing, addressing a critical challenge in polydisperse droplet dispensing. The platform enables highly accurate (99.9%) and high-throughput dispensing (up to 8,640 droplets per hour), effectively bridging droplet-based high-throughput screening assays with traditional biological workflows. Its utility was demonstrated in an antimicrobial susceptibility test, where resistant strains were successfully identified with high accuracy.

As featured in:

See Arum Han *et al.*,
Lab Chip, 2025, **25**, 6157.

ROYAL SOCIETY
OF **CHEMISTRY**

rsc.li/loc

Check for updates

Size-independent and automated single-colony-resolution microdroplet dispensing

Haemin Jung, [iD]†[a] Han Zhang, [iD]†[a] Jacob Hooper,[b] Can Huang, [iD][a] Rohit Gupte,[c] Adrian Guzman,[a] Jeong Jae Han[d] and Arum Han*[ace]

Droplet microfluidics-based high-throughput screening (HTS) has proven to be an effective method for rapidly analyzing broad ranges of biological samples, such as cell libraries. However, the final step of the droplet microfluidics-based screening workflow, which is to dispense the sorted "hit" droplets to off-chip, ideally one "hit" droplet at a time, is prone to high error, especially when droplet size variation is present. Such size variations, often unavoidable in complex multi-step droplet microfluidics assay, lead to variations in droplet transition speed as they flow towards the dispensing tip, where smaller droplets move faster than larger droplets within a microchannel. Such difference in transit speed causes simultaneous dispensing of multiple droplets at a time instead of single-droplet dispensing, resulting in "hit" cells in a dispensed droplet being mixed with those from another "hit" droplet. To address this challenge, an approach that uses blank spacing droplets as physical barriers between "hit" droplets so that "hit" droplet-to-droplet distance remains the same throughout the droplet transition process is proposed here. These blank droplets (up to 1000) and a single "hit" droplet flow out of the droplet dispensing tip, forming a "drip", which is then dispensed one "drip" at a time into a well of a well plate or on an agar plate with sufficient drip-to-drip distance. This method of mixing empty droplets with "hit" droplets, combined with an off-the-shelf distance sensor that detects the formation of a "drip", which then moves the dispensing plate upward using a linear motor for the formed "drip" to be dispensed, enables precise and automated single-drip (i.e., one "hit" droplet) dispensing even with polydisperse droplets. The developed system demonstrated a droplet dispensing accuracy of 99.9%, with a throughput of up to 8640 single drips (i.e., single "hit" droplets) per hour. The system's effectiveness was demonstrated through a droplet microfluidics-based antimicrobial susceptibility test (AST) assay, where four resistant strains from a mixture of 11 strains could be successfully identified. By smoothly transitioning droplet-encapsulated samples of interest identified through high-throughput droplet microfluidics assays to traditional biological assay workflow, this system offers a highly efficient, accurate, and cost-effective solution for conducting complex droplet microfluidics-based assays followed by further off-chip assays.

Introduction

Droplet microfluidics, where water-in-oil emulsion droplets serve as miniature bioreactors, enable high-throughput biological assays, especially at single-cell resolution.[1] Advances

[a] Department of Electrical and Computer Engineering, Texas A&M University, College Station, Texas 77843, USA. E-mail: arum.han@ece.tamu.edu
[b] Department of Epidemiology, Texas A&M University, College Station, Texas 77843, USA
[c] Department of Biomedical Engineering, Texas A&M University, College Station, TX 77843, USA
[d] Department of Multidisciplinary Engineering, Texas A&M University, College Station, TX 77843, USA
[e] Department of Chemical Engineering, Texas A&M University, College Station, TX 77843, USA
† These authors contributed equally to this work.

in droplet manipulation technologies, such as droplet generation, splitting, counting, merging, solution injection, and sorting[2–9] have facilitated increasingly complex assays across diverse applications, including drug discovery,[10–12] tissue engineering,[13,14] medical diagnostics,[15–17] and single-cell studies.[18–21] The final step of this assay is to dispense the "hit" droplets from the droplet microfluidic assays to an off-chip format for sample recovery and further analyses, which is typically conducted by dispensing the sorted "hit" droplets onto agar or multi-well plates. This enables the subsequent assays to be compatible with traditional biological assays. However, a critical challenge is to dispense the "hit" droplets without any of the "hit" droplets being mixed and cross-contaminated during this step.

The most basic method of droplet dispensing (Fig. 1a) is through manual streaking onto an agar plate, where tubing
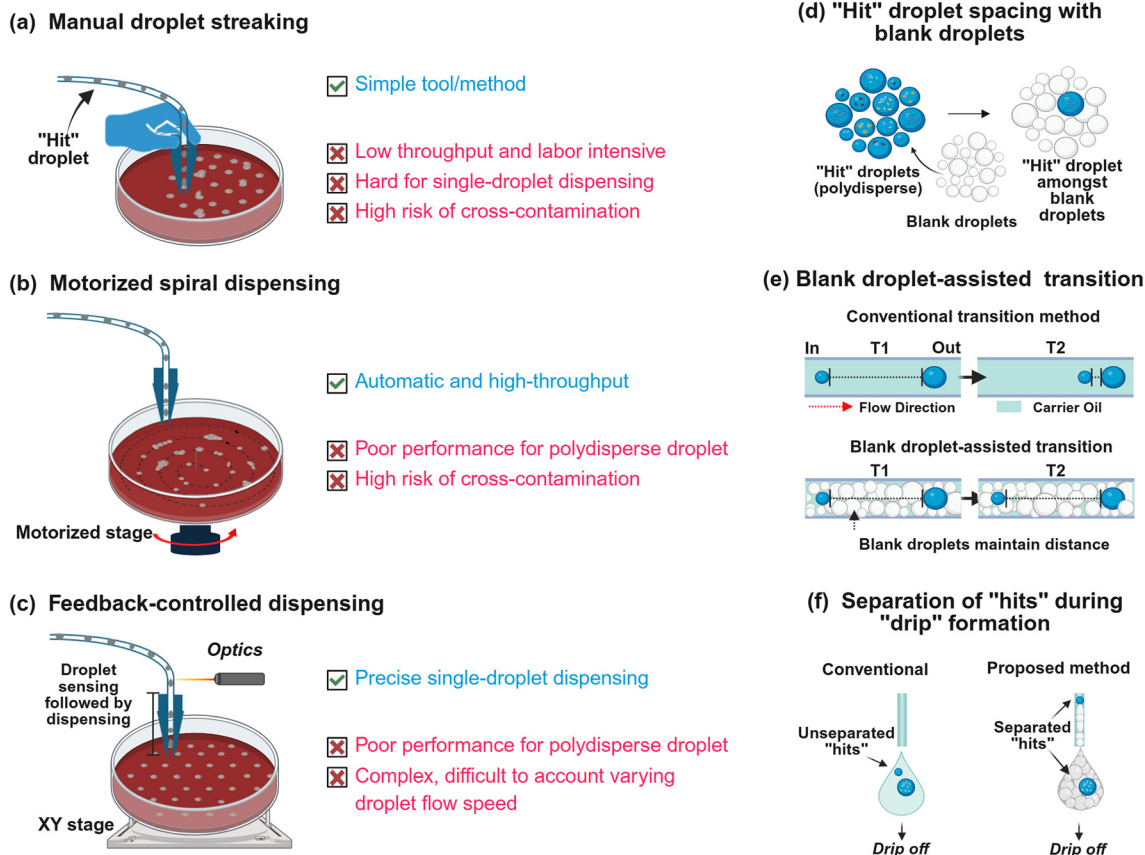
Fig. 1 Developed feedback-controlled blank spacing droplet-assisted droplet dispensing method compared to conventional methods. (a–c) Advantages and disadvantages of commonly used droplet dispensing methods. The proposed method includes three features: (d) mixing of "hit" droplets with a large number of blank spacing droplets to ensure enough spacing between the hit droplets so that the chance of more than one "hit" droplet being dispensed at a time is minimal. (e) The use of blank droplets ensures "hit" droplet-to-droplet distance is maintained during droplet flow through a tubing, especially in the case of polydisperse droplet population, while using only oil as a spacer will result in droplet-to-droplet distance to change over time; (f) the use of blank droplets further minimizes the chance that more than two "hit" droplets are present in a single drip since the "hit" droplet-to-droplet distance can be maintained when using blank droplets, especially when droplet sizes are polydisperse. Fig. 1/panels (A–D), created with **https://BioRender.com**, released under a Creative Commons Attribution-NonCommercial-NoDerivs 4.0 International license.

or other capillary devices containing the "hit" droplets deliver a stream of droplets onto an agar plate.[22] While being the simplest form of droplet dispensing, they fail to offer precise spatial control of the dispensed droplets, often leading to cross-contamination between the droplet contents. Motorized dispensing systems (Fig. 1b) reduce this manual effort. Thus, several studies have introduced motorized droplet dispensing systems.[23,24] While these approaches alleviate operator workload, such methods still lack precise control over individual droplets and their exact dispensing locations. Also, when droplet sizes are polydisperse, droplets travel at different speeds, making it challenging to control the droplet-to-droplet distances, resulting in cross-contamination between droplet contents. To address these challenges, some methods have incorporated droplet sensors near the dispensing tip to detect incoming droplets before dispensing (Fig. 1c), allowing precise positioning of individual droplets.[25–27] However, such methods require precise control of individual droplets along the dispensing tip, necessitating

either a complex feedback loop integrating a pressure controller for flowing the droplets, individual droplet sensing at the tip of the dispenser, and a motorized stage that controls the dispensing. A dielectrophoretic (DEP) sorting scheme at the tip of the dispensing tip to selectively eject only the desired droplets has also been developed.[27,28] However, such systems typically require complex integration of optical and electrical systems, increasing the system's complexity and cost.

One of the biggest challenges in most of these developed systems is that their performance drops significantly when the input droplets are polydisperse in size. Such polydispersity is oftentimes unavoidable as the uniformity of droplet size can be significantly compromised after multiple stages of droplet incubation and manipulation steps, such as cultivation, merging, and sorting.[29,30] The most critical determining factor of droplet dispensing at single-droplet resolution is the system's ability to space out the incoming input droplets to physically separate them onto the substrate onto which

droplets are dispensed. However, when the incoming input droplets are polydisperse in size, such systems fail to maintain the physical spacing between droplets since smaller droplets travel faster than larger droplets in a microchannel or tubing; thus, spacing between droplets cannot be maintained. Such difference in travel time within a microchannel makes the exact traveling time of individual polydisperse droplet populations almost impossible to factor into the droplet dispensing speed, resulting in more than one target droplet being dispensed simultaneously. This difference can be avoided by having a single droplet in transition from the droplet library to the droplet dispensing tip; however, this significantly affects the dispensing throughput due to the method requiring a substantial droplet-to-droplet spacing (easily in several tens of millimeters). A comprehensive summary of published dispensing results is provided in Table S1. While several commercially available reagent and droplet dispensing methods exist, none are designed to dispense discrete droplet samples, highlighting the distinctiveness of the proposed system.

Here, we present a high-precision, single-droplet-resolution dispensing method that is robust to input droplet size variation. The developed system employs blank droplets, either polydisperse or monodisperse, as spacers between target droplets, where the blank droplets act as a physical barrier between each target droplet flowing through a channel or tubing towards the dispenser tip, retaining the physical distance between each "hit" droplet. Then, during dispensing, a single "hit" droplet is dispensed together with hundreds of such blank spacer droplets, here defined as a "drip". The blank droplets dispensed on plates when a "drip" is dispensed also prevent the "hit" droplets from moving around, preventing cross-contamination between "hit" droplets after they are dispensed. Since a complex feedback control is not needed, this significantly reduces the system and operational complexity. The dispensing characteristics under various operating conditions, including flow rates, input droplet sizes, polydispersity, and mixing ratios between the "hit" and spacing droplets, have been thoroughly tested to characterize the system's resilience to polydisperse input droplet population. Finally, the developed "hit droplet" dispensing method was applied to a droplet microfluidics-based antibacterial susceptibility test (AST) assay as a demonstration case. This method offers broad applicability for sample retrieval following any droplet microfluidics-based screening assay by effectively bridging the gap between droplet microfluidics and conventional biological assay technologies.

Results and discussion

Working principle of the droplet dispensing system

Fig. 1d left depicts a typical input "hit" droplet library, comprising of small (disrupted), medium (original and unaltered), and large (unintentionally coalesced) droplets, ready to be dispensed to off-chip. This polydisperse droplet population is mixed with a large number of polydisperse blank droplets at a ratio of approximately 1 to 1000 so that when a group of droplets that we define as a single "drip" is dispensed, there is only a single "hit" droplet amongst many blank droplets. Although the illustration depicts the use of polydisperse blank droplets that can be generated in large numbers through a simple sonication process (equivalent to 20 000 droplets per s), monodisperse blank droplets generated through droplet microfluidic generators (up to 8000 droplets per s (ref. 31)) can also be used. These blank droplets help space out "hit" droplets as they flow through a flow channel or tubing toward a dispensing nozzle since they act as physical barriers between the "hit" droplets, maintaining the distance between the "hit" droplets (Fig. 1e bottom). In contrast, conventional spacing enabled through oil fails to maintain such distances since small droplets flow faster and eventually catch up with larger droplets (Fig. 1e top), leading to the dispensing of multiple "hit" droplets. The additional advantage of using blank droplets rather than carrier oil for droplet-to-droplet spacing during the drip formation process is shown in Fig. 1f. As droplets accumulate at the dispensing needle tip, they form a "drip" until sufficient volume is reached for gravitational force to overcome surface tension, resulting in drip detachment. This accumulation phase presents a critical challenge for traditional oil-based spacing methods, which fail to maintain consistent separation between "hit" droplets. In contrast, the developed method ensures that each "hit" droplet maintains the intended spacing according to the predetermined mixing ratio between the "hit" droplets and the large number of blank droplets, thereby preserving consistent "hit" droplet distribution throughout drip formation.

Dispensing characterization

The effect of blank spacer droplets on single "hit" droplet dispensing onto agar plates is shown in Fig. 2, providing a visual comparison to conventional methods. Various "hit" droplets were mixed with equal volumes of blank droplets and loaded into a syringe to test different hit-to-drip ratios (HDR). Here, HDR is defined as the number of "hit" droplets loaded into a syringe divided by the number of dispensed drips; in other words, how many "hit" droplets are in a single drip. Fig. 2a illustrates the mixing procedure at HDR = 1, where one "hit" droplet is present amongst 100–1000 blank droplets in a single drip. Typically, 1 mL sample volume generates around 800 drips when dispensed using a 23-gauge needle (inner diameter: 0.337 mm) onto an agar plate, where the volume of each drip ($\sim$0.1 μL) exhibits a relative standard deviation of 10.2% (n = 10). Notably, hydrophobic treatment of the needle surface can significantly influence the number of drips produced, with increased surface hydrophobicity allowing for smaller volumes to be suspended from the tip before it drips. The experiments in this study were conducted with a hydrophobically treated needle as the dispenser tip by applying AquaPel (PGWAG, LLC, PA, USA) coating to the inside and outside of the needle tip. Fig. 2b depicts black-
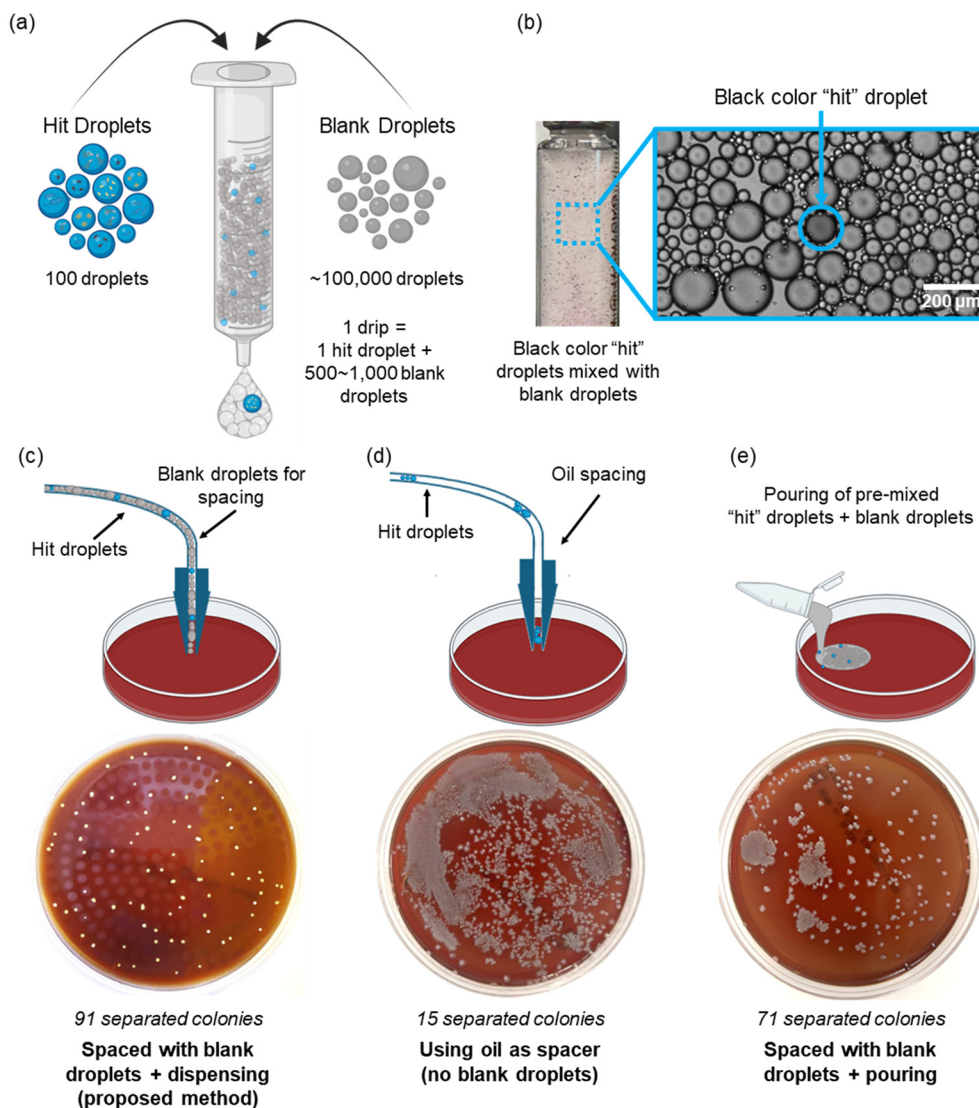
Fig. 2 Comparison of the developed blank droplet-assisted "hit" droplet spacing to conventional methods. (a) Mixing of "hit" droplets with a large number of blank droplets into a syringe. One drip ideally contains only a single "hit" droplet with a large number of blank droplets, where the HDR = 1. (b) Uniform mixing of polydisperse "hit" droplets (black color ink), used for easy visual confirmation, in large number of blank droplets. (c–e) Dispensing of *E. coli DH5α* cell-containing "hit" droplets onto a blood agar plate. (c) Developed blank droplet-assisted droplet spacing and dispensing (number of separated colonies formed = 91). (d) Oil as a spacer between droplets. Significantly more colonies are formed (number of separated colonies formed = 15) (e) use of blank droplets as spacers but directly pouring onto an agar plate rather than spacing out the "hit" droplets in a tubing and then dispensing. Improved compared to the use of an oil spacer, but still significantly more colonies were formed (number of separated colonies formed = 71). Fig. 2/ panel (A), created with **https://BioRender.com**, released under a Creative Commons Attribution-NonCommercial-NoDerivs 4.0 International license.

colored "hit" droplets mixed in a large number of blank droplets within a syringe. The results using conventional spacer oil-based droplet transition and the developed blank droplet-spaced transition method are compared in Fig. 2c. With the same number of input droplets containing *Escherichia coli DH5α*, 91, 71, and 15 separated colonies were observed for the respective methods. These results clearly show that dispensing droplets with blank spacing droplets yields optimal separation between each "hit" droplet, and thus, once "hit" droplets containing bacteria are cultivated on the dispensed agar plates, individual colonies are formed (Fig. 2c–e). In contrast, dispensing "hit" droplets with oil spacing results in "hit" droplets undergoing demulsification

upon contact with the substrate before the oil phase evaporates. This phenomenon results in the release and dispersal of the encapsulated bacteria, forming far more colonies on the plate than desired (Fig. 2d). Also, if the "hit" droplets mixed with a large number of blank droplets are poured directly onto an agar plate without tubing-based dispensing, individual "hit" droplets are not guaranteed to be separated from each other. This results in the growth of colonies that overlap with each other compared to the developed tubing-based dispensing method (Fig. 2e). Although significantly better than using an oil spacer, there are still many instances where the "hit" droplet contents are mixed, forming more colonies than the number of "hit"

droplets. Especially, when the "hit" droplets are not spaced out using blank droplets, a large number of overlapping colonies are seen, requiring additional off-chip processes to isolate a single strain. Although the same concentration of input droplets was used, Fig. 2d and e show a higher number of visible colonies compared to Fig. 2c. This is due to demulsification of droplets stemming from oil evaporation, which caused wider dispersal of bacterial cells from each droplet. The use of blank droplets is critical in mitigating this effect, as they help maintain droplet integrity and spatial localization during the transition from oil to agar. In summary, implementing blank spacer droplets for droplet dispensing significantly enhances the precision and reliability of the droplet dispensing process.

To confirm that the blank droplet-based spacing method maintains "hit" droplet distances during droplet transition, the distance between two "hit" droplets was monitored as they flow through a serpentine microfluidic channel. Here, to simulate realistic conditions, a serpentine microfluidic channel with dimensions of 200 μm width × 200 μm height (Fig. S1) was utilized, which is similar to a typical tubing inner dimension used in droplet microfluidic applications. In the blank droplet-based spacing method, the distance between the black-colored "hit" droplets (300 μm diameter) did not reduce even after the droplets traveled more than 10 mm (Fig. 3a left). In contrast, the conventional oil-based droplet spacing method reduced the gap between the small and large "hit" droplets to under 50 μm (from an initial

spacing of 300 μm) after traveling for less than 1 mm (Fig. 3a right). These results demonstrate that blank droplets can effectively maintain spacing between the "hit" droplets. The "hit" droplets in a drip were then dispensed on a slide glass substrate and imaged (Fig. 3b, each "hit" droplet highlighted with a red circle). Here, the blank droplet-assisted method only contained a single black-colored "hit" droplet (Fig. 3b left), whereas the oil-assisted method contained more than 10 "hit" droplets (Fig. 3b right). This result highlights the differences in "hit" droplet distribution per drip between the two approaches, where the conventional oil-assisted method resulted in the simultaneous dispensing of multiple "hit" droplets (simulated by black color droplets). In contrast, the developed blank droplet-based spacing method resulted in only a single "hit" droplet to dispense in a single drip.

Droplet handling during mixing and transition in tubing, as well as during dispensing, can cause physical disruption to droplets, which can result in the mixing of two different droplet contents (in the case of droplet merging) or a single droplet content to spread into multiple droplet contents, thus making the overall system inefficient. Systematic analyses using four distinct droplet size populations (40, 60, 80, and 100 μm diameter "hit" droplets) were conducted to evaluate the impact of these physical forces on droplet integrity. These "hit" droplets were mixed with polydisperse blank droplets and subjected to the entire dispensing workflow. As shown in Fig. 3c, rates of droplet merging during transition were 3.0%,
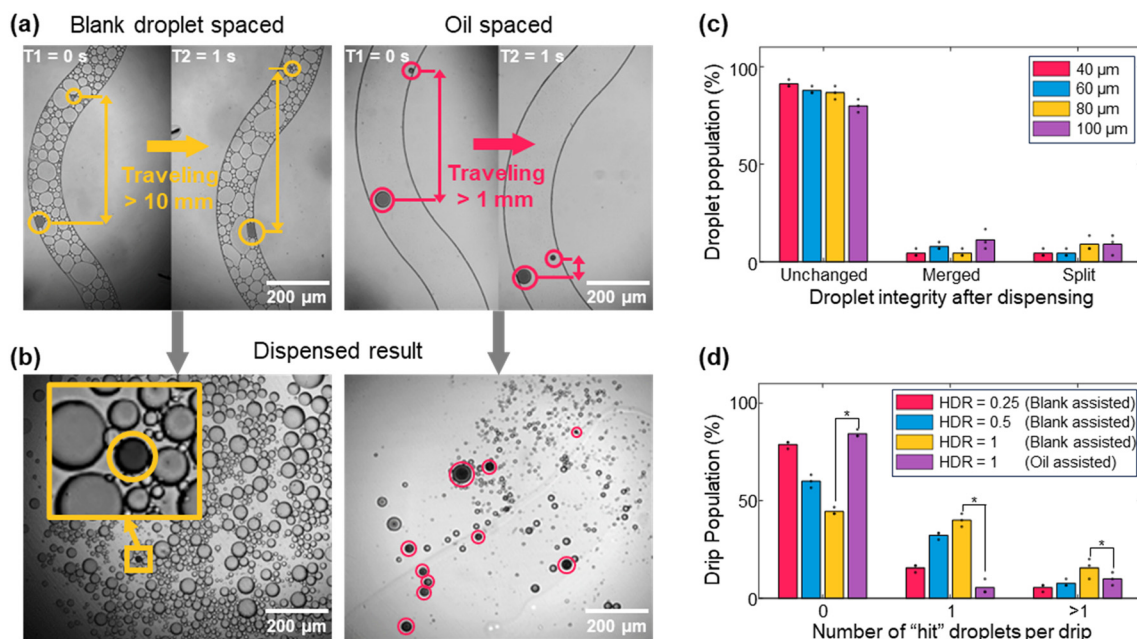

Fig. 3 Characterization of blank droplet-spaced droplet dispensing compared to conventional methods. (a) Impact of blank droplet-assistant droplet transition (left) *vs.* conventional oil-assisted droplet transition (right) on maintaining droplet-to-droplet distances of black color dye "hit" droplets. (b) Images of a single drip containing black-colored "hit" droplets. Left: Blank droplet spaced, where only a single black color dye "hit" droplet is observed; Right: Oil spaced, where multiple black color dye "hit" droplets are observed. (c) Effect of the "hit" droplet size on their integrity after blank droplet mixing and dispensing. *T*-test shows no statistical difference between all droplet sizes ($P > 0.05$). (d) The number of colonies formed at various HDRs, with and without blank spacing droplets. Three replicates were performed for each condition, and 30 drips were analyzed for each replicate.

8.0%, 4.3%, and 7.7%, and droplet splitting during transition were 2.7%, 3.3%, 10.0%, and 7.7%, respectively (40, 60, 80, and 100 μm diameter "hit" droplets). Here, droplets with more than 10% variance from their original size were considered either merged or split. These results show that increases in droplet size cause physical instability of droplets, where smaller droplets reduce the overall error rate.

Even though HDR is calculated as the hits-per-drip ratio at the blank droplet addition stage, HDR = 1 does not necessarily mean that there is only one hit droplet per drip due to the randomly mixed sample. A higher HDR increases the probability of multiple "hit" droplets per drip while also increasing the probability of more than one "hit" droplet being included in a single drip. In contrast, a lower HDR reduces the likelihood of multiple "hit" droplets in a single drip but increases the distance between each droplet, resulting in more empty drips and reducing the overall system throughput. Thus, the effect of HDR on the number of "hit" droplets per drip dispensed was investigated (Fig. 3d). At HDR = 1, 44.7% of drips contained a single "hit" droplet, 39.7% contained multiple "hit" droplets, and 15.7% were empty. At HDR = 0.5, the percentage of empty drips increased to 60.7%, while only 6.7% contained multiple "hit" droplets. At HDR = 0.25, the proportion of empty drips further increased to 78.7%, with just 5.3% containing multiple "hit" droplets. In contrast, the conventional oil spacing method yielded 85.0% empty drips, 4.3% single "hit" droplets per drip, and 10.7% multiple "hit" droplets per drip. Thus, a lower HDR should be employed if sample separation is critical. In contrast, if a small number of overlapping "hits" is tolerable, as they can always be separated during an off-chip validation step, a higher HDR may be used to increase the overall throughput of the assay. From here on, all following experiments were performed at HDR = 0.5. Due to the limited sample size (n = 3), formal statistical testing was not performed, as it would not provide meaningful inference. Instead, the data are presented with appropriate measures of variability to transparently reflect experimental trends.

Integration of a drip size detection sensor

Having only a single "hit" droplet in a single drip is determined by the HDR (as characterized above) and by the consistency in drip formation at the end of the dispensing tip. Since individual drip forming time varies and the "hit" droplets flow into the dispensing tip at a constant speed, this can result in a different number of "hit" droplets in each drip. Detecting a "hit" droplet using an optical sensor (similar to the ones used for fluorescence droplet sensing and sorting) complicates the overall setup. Instead, a simple distance sensor was integrated to monitor individual drips
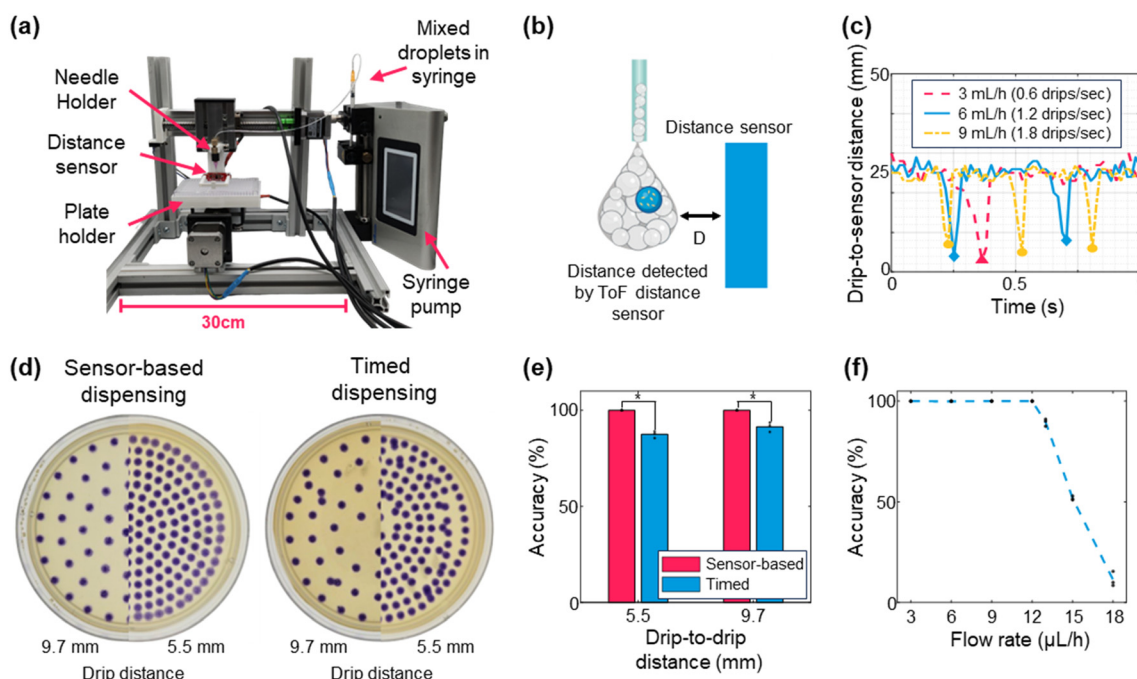

Fig. 4 Characterization of the drip sensing method using ToF distance sensor. (a) Image of the dispensing stage, highlighting the key components of the system. (b) Working principle of the distance sensor-based drip formation sensing. The sensed distance is reduced as a drip is formed, then rapidly goes back to the original sensor value, until another drip is formed. (c) Measured signal from the distance sensor during dispensing at different flow rates. (d) Images of agar plates onto which drips containing black color dye "hit" droplets are dispensed, using sensor-actuated drip dispensing (left) and fixed-time dispensing (right). (e) Accuracy of each drip position between sensor-actuated drip and timed methods. Three individual plates were analyzed after dispensing each at two different drip distances. A total of 173 (5.5 mm) and 62 (9.7 mm) drips were analyzed, * means $P < 0.05$. (f) Dispensing accuracy of the sensor-actuated dispensing method at different flow rates. For each flow rate, 50 drips were analyzed, with three different batches of droplets. Fig. 4/ panel (B), created with https://BioRender.com, released under a Creative Commons Attribution-NonCommercial-NoDerivs 4.0 International license.

forming at the dispensing needle's tip (Fig. 4a). Fig. 4b illustrates the positioning of the distance sensor relative to the dispensing needle. As a drip begins to form in front of the sensor, the measured distance between the drip and the sensor decreases. Once the droplet reaches sufficient volume at the tip of the needle, gravity causes it to detach and fall onto the substrate. This process results from the gradual accumulation of fluid, where interfacial tension and gravitational force reach an equilibrium point that triggers droplet release. The volume of a single drip is empirically determined by measuring the number of drips required to dispense 1 mL of fluid. Once a drip is dispensed, the sensor reading returns to the original value. A simple commercially available infrared time-of-flight (ToF) distance sensor was utilized for the distance sensing, resulting in a simple, low-cost method of detecting individual drips. Fig. 4c shows the distance measurement result at three different flow rates, where an increased flow rate results in more drips forming within the same time period. It can also be observed that there is a slight variation in distances from drip to drip, indicating that the drip size varies. Fig. S3b shows that the average time variation during dispensing between drips is 29.8, 19.4, and 51.5 ms at 6, 12, and 18 mL h^{-1}, respectively.

Based on this result, the drip-to-drip distances were set to 9.7 mm or 5.5 mm. The dispensed black color dye "hit" droplets on the agar plate show that the drip sensing scheme allows each drip to be dispensed precisely at the desired position (Fig. 4d left). In contrast, inaccurate dispensing can be observed when the drips were dispensed at a constant interval without sensor-based feedback control due to individual drip-forming time variation (Fig. 4d right). Fig. 4e shows the accuracy of the individual drip position after dispensing, where the accuracy is defined as the ratio between a properly positioned drip to drips that missed the target position. Missed drips were defined as those not placed in the desired coordinate. For both drip-to-drip distances of 9.7 and 5.5 mm, 100% drip accuracy was achieved for the sensor-based dispensing, whereas 87.0% (9.7 mm) and 90.7% (5.5 mm) accuracy were observed for the timed method (constant time interval, in this case, set for dispensing every 1 s at 5 mL h^{-1}). This result demonstrates that individual drip sensing can significantly improve the accuracy of droplet dispensing, minimizing droplet content cross-contamination and/or mixing after dispensing. Fig. 4f shows the accuracy of dispensed drips at different flow rates (from 3 mL h^{-1} to 18 mL h^{-1}). The maximum dispensing rate at which over 99% accuracy could be achieved was 12 mL h^{-1}, corresponding to 2.4 drips per s (8640 drips h^{-1}). Beyond this throughput, dispensing accuracy significantly declined due to the current motor's inability to match the speed of incoming drips. Although the system dispenses up to 8640 drips per hour, the effective throughput depends on the HDR. At HDR = 0.5, around 61% of drips are empty, yielding approximately 3370 hit droplets dispensed per hour. Lower HDRs will further reduce the number of hits per hour but improve single-hit purity (*e.g.*, at HDR = 0.1, around 90% of

drips are empty, yielding approximately 864 hit droplets dispensed per hour). Therefore, HDR selection should be guided by the acceptable tolerance for multi-hit events *versus* the desired screening throughput. Presently, the dispensing speed is limited by the dispensing stage motor's movement speed. Future iterations using higher-speed motors may further optimize the maximum achievable throughput.

Further characterization of the dispensing system through microbial colony formation analyses

Biological system validation was performed using *Salmonella enterica*, encapsulated into droplets, and dispensed at HDR = 0.25. Fig. 5a shows an example of the droplet-dispensed blood and heart-infused agar (BHIA) plate after 12 h of incubation. The enlarged images show individual drips (hazy circle shows where a drip has been dispensed) with and without *S. enterica* cell-encapsulated "hit" droplets dispensed on the agar plate and cultured, where a dispensed drip-containing *S. enterica* cell forms a colony. The overall plate shows that most drips contain no more than one "hit" droplet, and in instances where multiple "hit" droplets are present within a single drip, most colonies remain spatially distinct due to the presence of blank droplets that provide physical spacing between "hit" droplets. In total, 97 colonies formed (out of 173 drips), and 91 colonies (93.8%) remained separated at sufficient distances. The recovery rate of "hit" droplets, defined as the ratio between the input "hit" droplets *versus* number of grown colonies, remained close to 100% under three different flow rates tested, and the drip accuracy at different flow rates remained nearly 100% for all the conditions (Fig. 5b). This result demonstrates that different flow rates do not significantly impact recovery rate or drip accuracy.

The impact of surfactant concentration on bacterial growth was also investigated since higher surfactant concentration results in higher droplet stability but may also negatively impact bacterial growth.[32] The effect of perfluoropolyether (PFPE) surfactant concentration on colony formation upon bacterial cell-encapsulated "hit" droplet dispensing is shown in Fig. 5c. When using *S. enterica*, higher surfactant concentration hinders colony formation after dispensing onto an agar plate, as the reduced "hit" droplet recovery rates can be seen. The system allows for variable drip-to-drip distances during dispensing (Fig. 5d right), allowing different drip distances to maximize the throughput of each plate while maintaining sufficient distance between individual colonies. A demonstration of the dispensed agar plate with varying drip distance is provided (Fig. 5d), where two different strains with different growth speeds are chosen to show that the system can be adjusted to maximize the throughput of a given "hit" population by allowing the maximum number of drips to be plated while maintaining sufficient distance between the drips. For slow-growing *Cellulosimicrobium cellulans*, a drip distance of 5.5 mm was chosen, while for the fast-growing *E. coli-DH5α*, the largest distance of 9.7 mm was chosen. Fig. S4 shows that
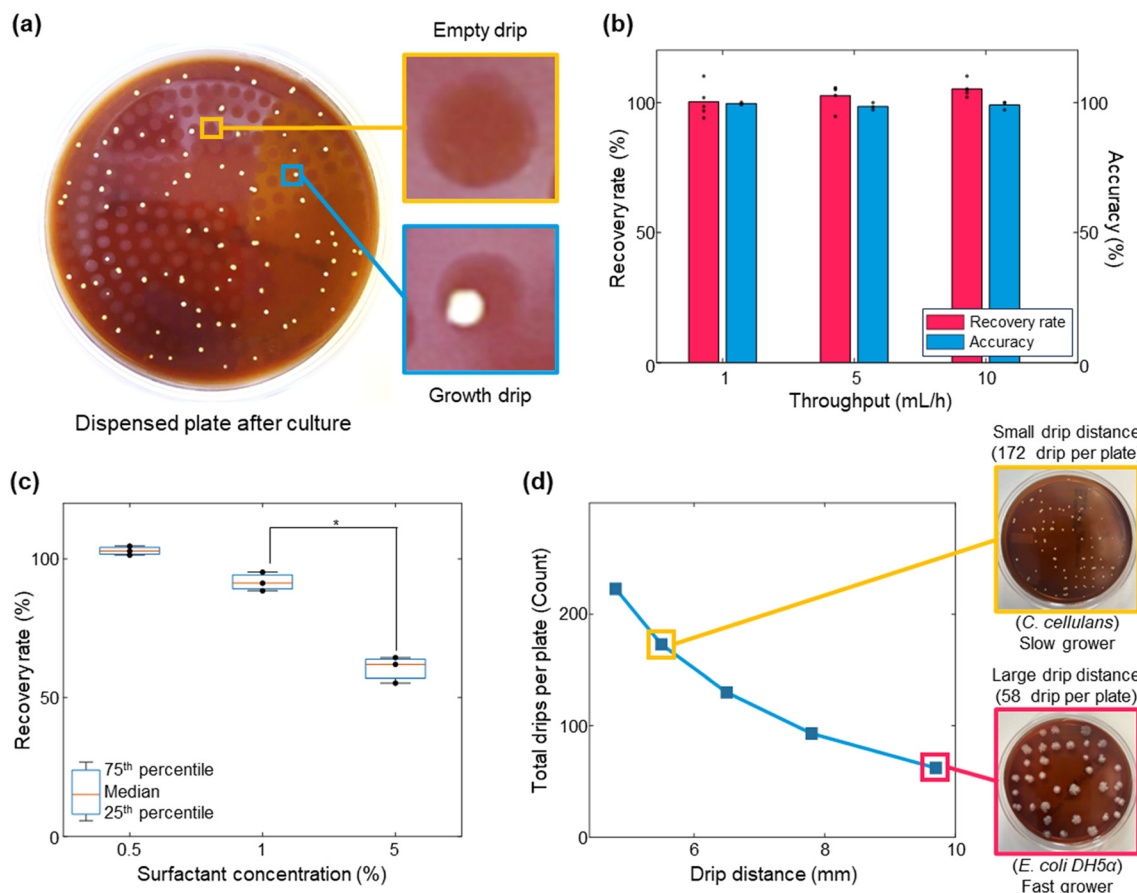
Fig. 5 Further characterization of the droplet dispenser through microbial colony formation analyses. (a) Dispensing of *S. enterica*-encapsulated "hit" droplets dispensed on a blood agar plate at TDR = 0.25 and then cultured for 12 h. Drips containing no "hit" droplets result in no colony formation, while drips containing a "hit" droplet forms a single colony. (b) Dispensing accuracy and recovery rate of hit droplets are shown after dispensing at different throughputs. Five plates for recovery rate and three plates were dispensed for each condition and then analyzed after incubation. *T*-test shows no statistical difference between all flowrates ($P > 0.05$). (c) The impact of surfactant concentration on the recovery rate of the "hit" droplets. Three individual plates, each having approximately 50–100 colonies were analyzed for each surfactant concentration after dispensing and 24 h culture, * means $P < 0.05$. (d) Number of drips that can be dispensed on a 10 cm diameter agar plate with respect to the distance between each drip. Different drip distances can be used depending on the presence of fast or slow grower in the population, where the images show the use of different drip distances when dispensing *C. cellulans* (slow grower, larger drip distance of 5.5 mm was used) and *E. coli* DH5α (fast grower, smaller drip distance of 9.7 mm was used) after 48 h culture (TDR = 0.5).

different dispensing patterns are achievable with the developed automated droplet dispenser. Although demonstrated using bacterial cells, the system is broadly compatible with a variety of cell types, including larger or more fragile ones such as mammalian or fungal cells, as long as they can be reliably encapsulated in droplets—a scenario supported by prior microfluidic studies. In fact, the droplet generator and dispensing component being used is in principle similar to many well-known droplet microfluidics device design that have been used for mammalian cell in-droplet cultivation and manipulation.[33–35] This compatibility further expands the system's applicability to diverse biological assays.

Applying the developed droplet dispenser in a droplet microfluidics-based antimicrobial susceptibility test (AST) assay

To demonstrate the utility of the developed droplet dispensing system, an antimicrobial susceptible test (AST)

assay was performed in droplet microfluidics format using a mock bacterial library composed of 11 common fast-growing model pathogens (Table S2) against the antibiotic ampicillin. These 11 strains were selected to cover both Gram-positive (total 4 strains) and Gram-negative (total 7 strains) bacteria having diverse ampicillin resistivity (4 resistant, 7 susceptive) for the proof-of-concept demonstration. Cell-encapsulated droplets were generated by co-encapsulating 50 μg mL^{-1} of ampicillin in lysogeny broth (LB) media with the bacterial library at single-cell resolution, followed by 24 h of in-droplet incubation for the clonal expansion of the encapsulated bacteria within the droplet. The incubated droplets were then dispensed onto BHIA plates using the developed droplet dispensing method, and then the plates were incubated for 12 h for colony formation. Fig. 6a summarizes the process of the assay. Colonies grown on the agar plates were randomly picked (91 total colonies) and sequenced to reconstruct the antimicrobial resistance profile of the tested microbial
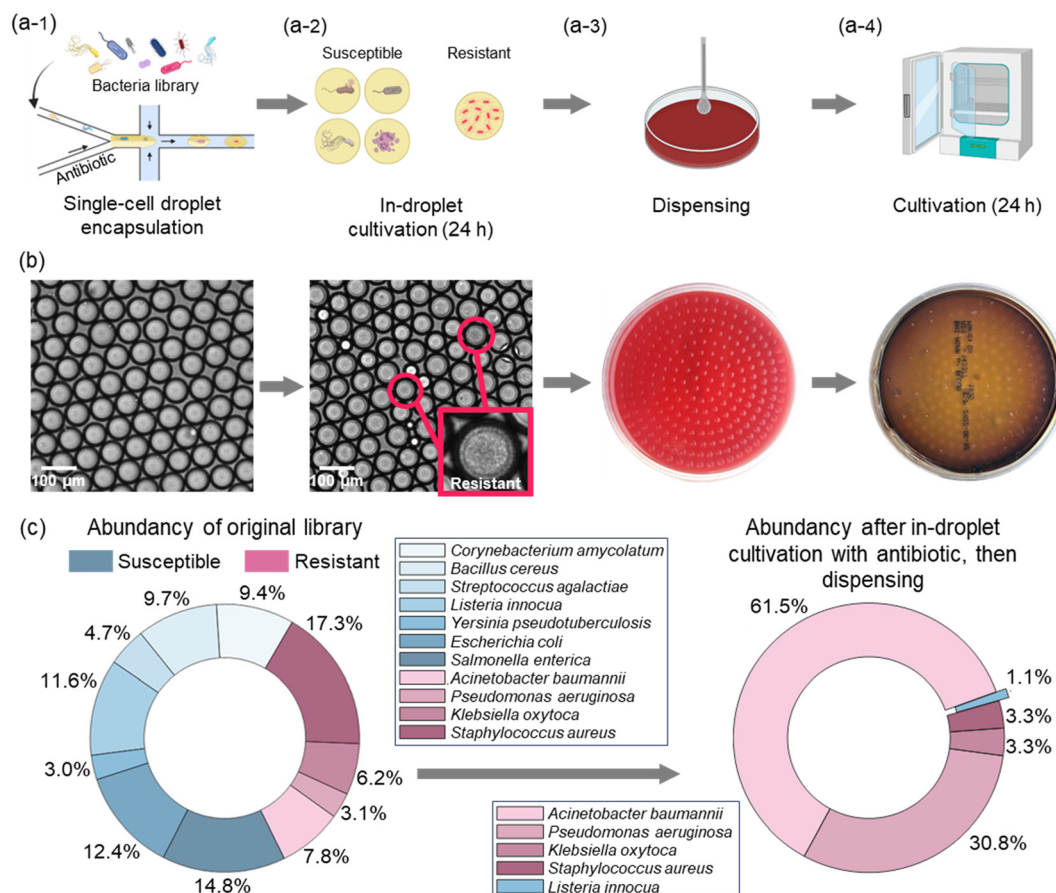
Fig. 6 Droplet microfluidics-based AST workflow and results. (a) Experimental overview of the in-droplet AST assay: (1) single-cell droplet encapsulation of bacteria with antibiotics; (2) in-droplet cultivation; (3) dispensing onto agar plates; (4) on-plate culture for colony formation. (b) Corresponding images of key steps of the illustrated workflow in "a". (c) Abundancy of the original 11 bacterial strain mix and the resulting abundancy after in-droplet AST testing. Fig. 6/panels (A and C), created with **https://BioRender.com**, released under a Creative Commons Attribution-NonCommercial-NoDerivs 4.0 International license.

consortia. Fig. 6b shows the corresponding images of the workflow illustrated in Fig. 5a.

Fig. 6c shows the relative abundances of the original input population (left graph, calculated based on colony forming unit [CFU] count) and the final harvested population (right graph) after in-droplet cultivation with ampicillin, followed by dispensing onto agar plates and then culture to until visible colonies were formed. The validation of 91 randomly picked colonies tested through 16 s rRNA sequencing revealed that among the original 11 strains, *Acinetobacter baumannii*, *Pseudomonas aeruginosa*, *Klebsiella oxytoca*, and *Staphylococcus aureus* exhibited resistance against 50 μg mL^{-1} of ampicillin treatment, as expected (4 resistant strains), and accounted for 98.9% of the final population compared to accounting for only 34.4% of the initial input population. Out of 91 sequenced colonies, 90 of them were from the originally identified resistant strains (56 being *A. baumannii*, 28 being *P. aeruginosa*, 3 being *K. oxytoca*, and 3 being *S. aureus*), with one exception being a *Listeria innocua* colony, which may be coming from cross-contamination. Also, the change in abundance amongst the 4 resistant strains before and after ampicillin treatment may be coming from their

differences in susceptibility to ampicillin. Compared to the other three resistant strains, *A. baumannii* strain exhibited exceptionally high ampicillin resistance, which could be why *A. baumannii* population was enriched after the in-droplet AST assay. A summary of the relative abundance of the eleven bacterial strains before and after the in-droplet AST assay is shown in Table S2.

Conclusion

This work addresses the challenge of dispensing polydisperse "hit" droplets selected from a droplet microfluidics screening assay onto an agar plate one "hit" droplet at a time to minimize cross-contamination while keeping the overall throughput high, a key limitation in current droplet dispensing methods. This paper introduces a method that uses blank spacing droplets to maintain physical separation between "hit" droplets throughout the entire dispensing process, ensuring single-droplet resolution handling. A distance sensor that can detect the formation of a "hit" droplet-containing "drip" and uses this information for feedback-controlled "drip" dispensing further improved the

accuracy of droplet dispensing by overcoming the variations in drip formation time. This method achieved 99.9% droplet dispensing accuracy, where most dispensed drips are positioned correctly, with a throughput of up to 8640 drips per hour (in an ideal condition this translates to a maximum of 17 280 "hit" droplets dispensed per hour when using HDR = 0.5), allowing an entire agar plate to be dispensed in less than one minute. Additionally, 94.3% of dispensed "hit" droplets remained intact. The blank spacer droplets also prevented "hit" droplets from moving around on the agar plate after dispensing, further minimizing the risk of cross-contamination between two different "hit" droplet contents. Demonstrating this method in a droplet microfluidics-based AST assay, the system successfully identified 4 resistant bacterial strains from a mixture of 11 strains, with a validation accuracy of 98.9%. This simple droplet dispensing method that is robust even with polydisperse input droplets offers a cost-effective, accurate, and robust solution suitable for a wide range of high-throughput droplet microfluidics biological assays, efficiently bridging droplet microfluidics with traditional biological assays.

Material and methods

Droplet microfluidics device fabrication

The droplet microfluidics device fabrication process employed a conventional soft lithography technique to create the microfluidic channel in polydimethylsiloxane (PDMS).[2,5,33,36–38] The individual droplet generator had channel heights of 30, 50, 70, and 90 μm, fabricated by first creating the master molds in SU-8™ 2035 for the 30 μm height microchannel devices and SU-8™ 2050 for the 50, 70, and 90 μm height microchannel devices. Each generator was used to generate 30, 50, 70, and 90 μm sized droplets to test the effect of different droplet sizes on the stability of droplets after dispensing. After the molds were fabricated, the surface of the molds was coated with tridecafluoro-1,1,2,2-tetrahydrooctyl-1-trichlorosilan (United Chemical Technologies, Inc., PA, USA) to facilitate PDMS layer release. Liquid-phase PDMS resin (Sylgard 184, Dow Inc., MI, USA) was mixed at a 10:1 ratio of base resin to curing agent and was poured onto the SU-8 master mold, cured for 30 min at 85 °C, and then subsequently released. The PDMS layer was bonded onto a 0.7 mm-thick borosilicate glass substrate after O_2 plasma treatment and then baked at 85 °C for 24 h.

Design of the feedback control-based droplet dispenser

The droplet-dispensing motorized stage comprises two linear motors, a drip dispensing needle holder, a plate holder, and a syringe pump, as shown in Fig. 4a. The two stepper motors whose shaft angle can be precisely controlled (17HE19-2004S, StepperOnline Inc., NY, USA) are connected to a linear rail, converting the rotary motion to a linear motion, allowing the precise control of the position of the plate. These linear rails are responsible for positioning the plate under the dispensing tip, enabling each drip to be positioned at each

location. Each motor is controlled using a stepper motor driver (DM542T, StepperOnline Inc., NY, USA), which is individually controlled by the main controller (Raspberry Pi 5, Raspberry Pi Foundation, Cambridge, UK) by series of pulse signals to indicate the position of each motor. The distance sensor (VL6180, SparkFun Electronics, CO, USA) is placed in front of the dispensing needle for drip detection. The sensor was spray-coated with an acrylic conformal coating (2108-12S, Techspray, GA, USA) to achieve watertightness. The drip signal acquired from the distance sensor is sent to the main controller *via* the I2C protocol, where the signal is processed using a moving mean filter to reduce noise. Then, the peaks of the signal are detected using a z-score-based peak detection algorithm.[39] These detected peaks trigger the linear motors to their subsequent position. The overall structure of the stage is assembled with aluminum extrusion bars, allowing for ease of assembly and sturdiness of the stage. The plate holder is printed with a 3D printer to allow dispensing onto agar and well plates.

All control electronics are separated from this motorized droplet dispensing stage to minimize the number of electronic components placed within a biosafety cabinet (Fig. S2c). Such design consideration allows a thorough decontamination process of the equipment in direct contact with biological samples, such as simple ethanol spraying or UV decontamination of all the components placed within the BSC. All the required power/signal connections are made through four wires connecting the motorized stage to the controller box through water-tight connectors. The controller box can be controlled with a touchscreen (Fig. S2d), where the user can select different plate types, either a well plate or an agar plate. Different droplet dispensing patterns or drip distances can be selected according to specific experiments. The syringe pump (Legato® 100, KD Scientific, MA, USA) is also connected to the controller box, minimizing the requirement for user intervention. The user interface (UI) and the control software were written with Python 3.5.10 and PyQT(Riverbank Computing Limited, UK). The functional schematic of the automated droplet dispenser, the operational flowchart, and the user interface (UI) of the droplet dispenser system are provided in Fig. S2. Detailed design methodology is discussed in the supplementary section.

Evaluation of droplet dispensing

Generation of blank droplets. Blank spacing droplets were generated using an off-chip method, where 1.5 mL of sterilized deionized (DI) water, 0.5 mL of NOVEC 7500 oil (3 M, Minnesota, USA), and 0.5%, 1%, and 5% Pico-surf-1 surfactant (Sphere Fluidics, Cambridge, UK) were directly added into a 3 ml syringe by withdrawing the syringe plunger. After all liquids were added, the syringe plunger was retracted to its limit and vortexed for 1 min, generating polydisperse water-in-oil emulsion droplets.

Generation of "hit" droplets. Seven different types of droplets were generated using the following methods: four

different-sized monodisperse, polydisperse black ink, and mono-disperse bacterial-encapsulated droplets. First, monodisperse black ink droplets were generated in four sizes (40, 60, 80, and 100 μm in diameter) using a microfluidic flow-focusing droplet generator.[2,5,36–38,40] Black ink was used as the aqueous phase, and NOVEC 7500 oil with 2% Pico-surf-1 was used as the oil phase. Second, polydisperse black ink droplets were generated using the same procedure as the blank spacing droplets using vortexing. However, 2% Pico-surf was used instead of 0.5% to increase droplet stability. It is worth noting here that the stability of the generated droplets is not significantly hindered by mixing with a droplet mix generated with a lower surfactant concentration. The bacteria-encapsulated droplets containing *E. coli DH5α*, *C. cellulans*, and *S. enterica* were prepared the following way. All strains were inoculated in the regular LB broth culture for 12 h from glycerol stock. The inoculated medium was flown through microfluidic flow-focus generators with NOVEC 7500 oil with 2% Pico-surf-1 to generate 60 μm diameter droplets. All generated droplets were collected in a plastic 1 mL syringe for usage.

Preparation of droplet mixture. The "hit" droplets were added to the syringe containing the blank spacing droplets. The amount of "hit" droplets added to the blank droplets was based on the chosen HDR. After the "hit" droplets were loaded into the syringe, the plunger was pushed so that there were minimal air bubbles within the syringe to minimize droplet disruption during mixing. The syringe was manually rotated along its longitudinal axis to perform droplet mixing while flipping it up and down. This mixing step was performed for 1 minute to ensure the mixing of droplets throughout the syringe was even and had minimal disturbance to the droplets.

Analyses of individual drips. The syringe containing the droplet mixture to be dispensed was loaded onto a syringe pump, and dispensing was performed onto a 96-well plate lid for easy droplet observation. This plate lid was prefilled with 2% NOVEC 7500 oil with 2% Pico-surf-1 to maintain the integrity of droplets for image analysis. When the dispensing was completed, each well was covered with a cover slide, and the internal volume was filled to remove any air bubbles. The well plate lid was then placed under an inverted microscope (Ti2-E, Nikon, Tokyo, Japan) for image acquisition. If size validation of the droplets is required, the images were analyzed with an image analysis pipeline developed in Matlab (Mathworks, Massachusetts, USA) to quantify each droplet size. Atherton and Kerbyson's phase-coding method[41] was employed to detect individual droplets' center and radius.

Droplet microfluidics-based antibiotic susceptibility test (AST)

Eleven bacterial strains (*Corynebacterium amycolatum*, *Bacillus cereus*, *Streptococcus agalactiae*, *L. innocua*, *Yersinia pseudotuberculosis*, *E. coli*, *S. enterica*, *A. baumannii*, *P. aeruginosa*, *K. oxytoca*, and *S. aureus*), including some known biosafety level 2 (BLS2) pathogen while covering both Gram-positive and Gram-negative, were mixed for bacterial library generation. The bacterial strains were kindly provided by the National Institute of Standards and Technology (NIST, USA) under the DARPA Cooperative Agreement W911NF1920013. All microbial strains were handled under biosafety level 2 (BSL-2) protocols approved by Texas A&M University. Each strain was first tested individually on both 50 μg mL^{-1} ampicillin LB agar plate and liquid LB culture to confirm their susceptibility to ampicillin. Four of the 11 strains were confirmed to be resistant to the given ampicillin concentration (*A. baumannii*, *P. aeruginosa*, *K. oxytoca*, *S. aureus*). When generating the 11-strain mixture, all 11 strains were inoculated in regular LB broth culture overnight and resuspended in fresh LB broth before mixing. Their OD$_{600}$ values were individually measured before mixing to calculate the resulting mixed concentration based on the existing OD *vs.* CFU to calculate the relative abundance of each strain within the mock library. Information regarding the individual strains, including gram+/−, strain ID, ampicillin susceptibility, and relative abundance, can be found in Table S2. Further, necessary dilution was taken with additional LB broth to calibrate the cell concentration to 5 × 10^6 CFU mL^{-1}, which is adequate for single-cell encapsulation with the target droplet size (60 μm diameter). Single-cell encapsulated droplets were generated with a conventional co-flow focusing droplet generator using the mock cell library mixture with 100 μg mL^{-1} ampicillin-containing LB at a mixing ratio of 1 : 1. The generated droplets were cultured at 37 °C for 24 h before dispensing. After the droplets had been cultured, the sample was mixed within a syringe and then dispensed onto a BHI agar plate, which was then cultured again at 37 °C for 24 h. The agar plates were first visually examined to confirm the formation of individual colonies. They were then randomly picked colonies to be sent for 16 s sequencing for strain confirmation, aiming to provide an approximate evaluation of the strains harvested and their relative abundance after such AST treatment. To maintain sterility, syringes were single-use, and tubing was either replaced or flushed with 70% ethanol followed by sterile DI water. All components in contact with biological samples can be sterilized using standard lab protocols. However, for real screening applications, using syringes and tubing only one time is desired, especially considering the low cost of these consumables.

Author contributions

Haemin Jung: conceptualization, methodology, validation, investigation, writing – original draft, writing – review & editing, data curation. Han Zhang: conceptualization, methodology, validation, investigation, writing – original draft, writing – review & editing, data curation. Jacob Hooper: data curation, validation, investigation. Can Huang: conceptualization, writing – review & editing, data curation. Rohit Gupte: data curation, writing – review & editing. Adrian Guzman: conceptualization. Jeong Jae Han: data curation. Arum Han: conceptualization, resources, writing – review & editing, supervision, funding acquisition.

Conflicts of interest

Data availability

Supplementary information: SI contains raw experimental data, extended datasets, and data analysis supporting the main findings of this study. See DOI: https://doi.org/10.1039/D5LC00374A.

Data for this article, including [figures or tables] are available at figshare at https://figshare.com/s/b84bf0ae83ecae212e5e.

Part of the data supporting this article have been included as part of the SI.

Acknowledgements

References

1 I. Kobayashi, K. Uemura and M. Nakajima, Formulation of monodisperse emulsions using submicron-channel arrays, *Colloids Surf., A*, 2007, **296**, 285–289.

2 B. Demaree, D. Weisgerber, F. Lan and A. R. Abate, An Ultrahigh-throughput Microfluidic Platform for Single-cell Genome Sequencing, *J. Visualized Exp.*, 2018, 57598, DOI: 10.3791/57598.

3 I. C. Clark and A. R. Abate, Microfluidic bead encapsulation above 20 kHz with triggered drop formation, *Lab Chip*, 2018, **18**, 3598–3605.

4 N. Sobahi and A. Han, High-throughput and label-free multi-outlet cell counting using a single pair of impedance electrodes, *Biosens. Bioelectron.*, 2020, **166**, 112458.

5 H. Zhang, *et al.*, FIDELITY: A quality control system for droplet microfluidics, *Sci. Adv.*, 2022, **8**, eabc9108.

6 H. Zhang, *et al.*, An ultra high-efficiency droplet microfluidics platform using automatically synchronized droplet pairing and merging, *Lab Chip*, 2020, **20**, 3948–3959.

7 A. R. Abate, T. Hung, P. Mary, J. J. Agresti and D. A. Weitz, High-throughput injection with microfluidics using picoinjectors, *Proc. Natl. Acad. Sci. U. S. A.*, 2010, **107**, 19163–19166.

8 C. Huang, Y. Jiang, Y. Li and H. Zhang, Droplet Detection and Sorting System in Microfluidics: A Review, *Micromachines*, 2023, **14**, 103.

9 M. Mastiani, B. Mosavati and M. Kim, Numerical simulation of high inertial liquid-in-gas droplet in a T-junction microchannel, *RSC Adv.*, 2017, **7**, 48512–48525.

10 G. Schneider, Automating drug discovery, *Nat. Rev. Drug Discovery*, 2018, **17**, 97–113.

11 M. Torabinia, U. S. Dakarapu, P. Asgari, J. Jeon and H. Moon, Electrowetting-on-dielectric (EWOD) digital microfluidic device for in-line workup in organic reactions: A critical step in the drug discovery work cycle, *Sens. Actuators, B*, 2021, **330**, 129252.

12 Y. Wang, *et al.*, Advances of droplet-based microfluidics in drug discovery, *Expert Opin. Drug Discovery*, 2020, **15**, 969–979.

13 S. Mashaghi, A. Abbaspourrad, D. Weitz and A. van Oijen, Droplet microfluidics: a tool for biology, chemistry and nanotechnology, *TrAC, Trends Anal. Chem.*, 2016, 118–125, DOI: 10.1016/j.trac.2016.05.019.

14 H. Yin and D. Marshall, Microfluidics for single cell analysis, *Curr. Opin. Biotechnol.*, 2012, **23**, 110–119.

15 K. Takeuchi, N. Takama, R. Kinoshita, T. Okitsu and B. Kim, Flexible and porous microneedles of PDMS for continuous glucose monitoring, *Biomed. Microdevices*, 2020, **22**, 79.

16 C. Chen, *et al.*, Novel Wax Valves To Improve Distance-Based Analyte Detection in Paper Microfluidics, *Anal. Chem.*, 2019, **91**, 5169–5175.

17 J. Dai, H. Zhang, C. Huang, Z. Chen and A. Han, A Gel-Based Separation-Free Point-of-Care Device for Whole Blood Glucose Detection, *Anal. Chem.*, 2020, **92**, 16122–16129.

18 T. Stuart and R. Satija, Integrative single-cell analysis, *Nat. Rev. Genet.*, 2019, **20**, 257–272.

19 M. D. Luecken and F. J. Theis, Current best practices in single-cell RNA-seq analysis: a tutorial, *Mol. Syst. Biol.*, 2019, **15**, e8746.

20 W. Stephenson, *et al.*, Single-cell RNA-seq of rheumatoid arthritis synovial tissue using low-cost microfluidic instrumentation, *Nat. Commun.*, 2018, **9**, 791.

21 D. W. Weisgerber, M. N. Hatori and A. R. Abate, Particle Templated Emulsification enables Microfluidic-Free Droplet Assays, *J. Visualized Exp.*, 2021, (169), DOI: 10.3791/62248.

22 L. Dong, D.-W. Chen, S.-J. Liu and W. Du, Automated Chemotactic Sorting and Single-cell Cultivation of Microbes using Droplet Microfluidics, *Sci. Rep.*, 2016, **6**, 24192.

23 C.-Y. Jiang, *et al.*, High-Throughput Single-Cell Cultivation on Microfluidic Streak Plates, *Appl. Environ. Microbiol.*, 2016, **82**, 2210–2218.

24 L. Mahler, *et al.*, Highly parallelized droplet cultivation and prioritization of antibiotic producers from natural microbial communities, *eLife*, 2021, **10**, e64774.

25 J.-C. Baret, *et al.*, Fluorescence-activated droplet sorting (FADS): efficient microfluidic cell sorting based on enzymatic activity, *Lab Chip*, 2009, **9**, 1850–1858.

26 T. Weber, *et al.*, Recovery and isolation of individual microfluidic picoliter droplets by triggered deposition, *Sens. Actuators, B*, 2022, **369**, 132289.

27 R. H. Cole, *et al.*, Printed droplet microfluidics for on demand dispensing of picoliter droplets and cells, *Proc. Natl. Acad. Sci. U. S. A.*, 2017, **114**, 8728–8733.

28 Y. Qin, *et al.*, A Fluorescence-Activated Single-Droplet Dispenser for High Accuracy Single-Droplet and Single-Cell Sorting and Dispensing, *Anal. Chem.*, 2019, **91**, 6815–6819.

29 R. Tu, *et al.*, Droplet-based microfluidic platform for high-throughput screening of Streptomyces, *Commun. Biol.*, 2021, **4**, 1–9.

30 R. He, R. Ding, J. A. Heyman, D. Zhang and R. Tu, Ultra-high-throughput picoliter-droplet microfluidics screening of the industrial cellulase-producing filamentous fungus Trichoderma reesei, *J. Ind. Microbiol. Biotechnol.*, 2019, **46**, 1603–1610.

31 J. Wu, S. Yadavali, D. Lee and D. A. Issadore, Scaling up the throughput of microfluidic droplet-based materials synthesis: A review of recent progress and outlook, *Appl. Phys. Rev.*, 2021, **8**, 031304.

32 S. Ki and D.-K. Kang, Gas Crosstalk between PFPE–PEG–PFPE Triblock Copolymer Surfactant-Based Microdroplets and Monitoring Bacterial Gas Metabolism with Droplet-Based Microfluidics, *Biosensors*, 2020, **10**, 172.

33 J. A. Wippold, *et al.*, PRESCIENT: platform for the rapid evaluation of antibody success using integrated microfluidics enabled technology, *Lab Chip*, 2020, **20**, 1628–1638.

34 S. Iftikhar, A. Vigne and J. E. Sepulveda-Diaz, Droplet-based microfluidics platform for antifungal analysis against filamentous fungi, *Sci. Rep.*, 2021, **11**, 22998.

35 B. Li, *et al.*, Droplets microfluidics platform—A tool for single cell research, *Front. Bioeng. Biotechnol.*, 2023, **11**, 1121870.

36 S.-I. Han, C. Huang and A. Han, In-droplet cell separation based on bipolar dielectrophoretic response to facilitate cellular droplet assays, *Lab Chip*, 2020, **20**, 3832–3841.

37 H. S. Kim, *et al.*, High-throughput droplet microfluidics screening platform for selecting fast-growing and high lipid-producing microalgae from a mutant library, *Plant Direct*, 2017, **1**, e00011.

38 S.-I. Han, H. Soo Kim and A. Han, In-droplet cell concentration using dielectrophoresis, *Biosens. Bioelectron.*, 2017, **97**, 41–45.

39 J. P. G. van Brakel, Robust peak detection algorithm using z-scores, Stack Overflow, 2014.

40 J. A. Wippold, *et al.*, XPORT ENTRAP: A droplet microfluidic platform for enhanced DNA transfer between microbial species, *New Biotechnol.*, 2024, **81**, 10–19.

41 T. J. Atherton and D. J. Kerbyson, Size invariant circle detection, *Image Vis. Comput.*, 1999, **17**, 795–803.